Phys. Status Solidi A **208**, No. 9, 2033–2037 (2011) / **DOI** 10.1002/pssa.201100007

physica status solidi a
www.pss-a.com
applications and materials science

Fabrication of adherent porous diamond films on sintered WC-13 wt.%Co substrates by bias enhanced hot filament chemical vapour deposition

Q. Wei[*,1,2,3], **M. N. R. Ashfold**[2], **Z. M. Yu**[1], **and L. Ma**[3]

[1] School of Materials Science and Engineering, Central South University, Changsha 410083, P.R. China
[2] School of Chemistry, University of Bristol, Bristol BS8 1TS, UK
[3] State Key Laboratory of Powder Metallurgy, Central South University, Changsha 410083, P.R. China

Received 20 February 2011, revised 1 May 2011, accepted 3 May 2011
Published online 10 August 2011

Keywords diamond films, HFCVD, porous, WC-Co

[*] Corresponding author: e-mail qpweicsu@gmail.com, Phone: +86 731 8830335, Fax: +86 731 8876692

Porous diamond (PD) films have been grown on sintered WC-13 wt.%Co substrates by bias enhanced hot filament (HF) chemical vapour deposition (CVD) methods and characterized by scanning electron microscopy (SEM), laser Raman spectroscopy and X-ray diffraction (XRD). The PD films show excellent adhesion under Rockwell indentation testing. Factors encouraging the growth of diamond film with high porosity are discussed.

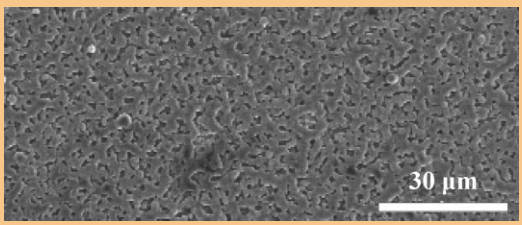

1 Introduction The exceptional properties of diamond, such as extreme hardness, low friction coefficient, physical and chemical stability, high electrical resistivity, wide band gap, semiconductivity when doped, broad UV, visible and IR transparency, high refractive index, the highest thermal conductivity at room temperature with a high Debye temperature and good biocompatibility, make it a very attractive material for a wide spectrum of applications in the fields of cutting tools, optical and electronic devices, etc. [1, 2]. Porous diamond (PD) films have received much recent attention [3–12]. The high surface area and multi-faceted morphology of PD films increases their capacity for electron field emission, and the aspect ratios of the emission sites [9]. Individual diamond grains can possess numerous micro-tips, many of which can sustain point discharges under an applied electric field. The increased surface area accompanying porosity can thus lead to increased field emission current densities and lower threshold voltages for field emission [10]. Conductive polycrystalline diamond films are also excellent candidate electrode materials, which can show a wide potential window, high corrosion resistance and enhanced mechanical stability relative to other commonly used electrode materials (*e.g.*, glassy carbon, graphite or platinum). Diamond films grown on porous anodic alumina have received particular attention, due to their (comparatively) low cost, large-area, controllable pore size and reliable fabrication [9].

We have recently reported hot filament (HF) assisted chemical vapour deposition (CVD) of adherent diamond films on steel substrates that had themselves been pre-coated with a thin WC-Co interlayer [13, 14]. Successful diamond growth was achieved after pre-treating the WC-Co interlayer with a two stage etching process, which had the effect of depleting the Co content at the surface. A range of pre-treatment methods for diamond films deposited on sintered WC-Co substrates with different cobalt contents have also been investigated [15, 16]. Here, we report growth of adherent PD films on sintered WC-13 wt.%Co substrates by bias enhanced HF CVD methods, and explore their morphological and mechanical properties as functions of

selected deposition parameters (surface pre-treatment, bias conditions and input gas mixture).

2 Experimental details PD films were prepared on sintered WC-13 wt.%Co substrates using an HFCVD reactor, the details of which have been reported previously [13, 17]. Briefly, the reactor is a stainless steel chamber (300 mm inner diameter) to which are fitted various electrical, gas and liquid feed-throughs, as well as a magnetron cathode for sputtering. The process gas was activated using a spiral coil filament (tungsten wire, diameter 0.38 mm, screw inner diameter 1 mm, 14 turns, 1 mm separation between adjacent turns, coil length 14 mm), suspended between two molybdenum rods that are themselves mounted on water cooled copper frames. The filament temperature (T_f) was measured by optical pyrometry. A linear motion feed-through allowed *in situ* control of the filament-substrate distance (d_f), which in the present work was maintained at ~8 mm. The substrate temperature (T_s) was controlled by T_f and d_f, and measured by K-type thermocouples attached to the substrate surface. The base pressure ($<1 \times 10^{-6}$ Torr) was maintained by a turbomolecular pump, and the deposition pressure (p) monitored and controlled using a manometer. Deposition parameters were varied in the range: filament power, $P = 361$–394 W; filament current, $I = 19.3 \pm 0.2$ A; $T_f = 2100 \pm 100$ °C; $p = 4$ kPa; $T_s = 750 \pm 10$ °C; methane and argon mole fractions, $C_m = 3\%$ and $C_a = 4\%$, respectively, in hydrogen; total flow rate, $F_g = 60$ standard cm^3 per min (sccm); deposition time, $t = 200$ min. Bias voltages were applied directly to the substrate through the molybdenum substrate holder. For the studies reported here, an initial negative bias of -150 V was employed during the period $0 \le t \le 15$ min. This was followed by 30 min of growth without any bias, then 60 min deposition with a positive bias of $+100$ V, and finally 95 min deposition without any bias.

Sintered WC-13 wt.%Co plates (Zhuzhou Cemented Carbide Group Corporation, Hunan, China) with dimension of $6 \times 6 \times 3$ mm^3 were used as substrates. These were first subjected to the following two-step MC (Murakami reagent and Caro acid) pre-treatment [16, 18]: (i) etching of tungsten carbide by Murakami's reagent (10 g $K_3[Fe(CN)_6]$ + 10 g KOH + 100 mL H_2O) for 30 min in an ultrasonic vessel; (ii) removal of the surface Co by etching in an acidic solution of hydrogen peroxide (3 mL 96 wt.% H_2SO_4 + 10 mL 40% w/v H_2O_2) for 30 s. Prior to diamond deposition, all pre-treated specimens were then abraded ultrasonically in a suspension of detonation nanodiamond powder (~500 nm) in acetone for 30 min. Ultrasonic agitation serves to disperse the nanodiamond powder in the acetone and to enhance collisions of diamond particles with the substrate surface, seeding the subsequent inhomogeneous nucleation of diamond during CVD [19, 20] by implanting ultrafine diamond fragments into the substrate surface and/or by creating suitable surface defects. The substrate samples were subsequently cleaned ultrasonically with acetone and ethanol for 3 min after the seeding treatment.

Samples were characterized with field-emission scanning electron microscopy (FE-SEM FEI, Sirion200), X-ray diffraction (XRD: Dmax-2500VBX using Cu K_α radiation at a wavelength of 0.154 nm) and Raman spectroscopy (LabRAM HR800, Ar^+ ion laser operating at 488 nm with an output power of 100 mW). The mechanical properties of the diamond-coated WC-Co substrates were characterized using a Rockwell hardness tester with a Brale diamond indenter (angle = 120°, radius = 0.2 mm) at loads of 600, 1000 and 1500 N.

3 Results and discussion Figure 1 shows representative cross-section and surface SEM images of a PD film deposited using the above conditions on a sintered WC-13 wt.%Co substrate. Cross-sectional analysis post-indentation testing was performed after polishing the samples with diamond abrasive paste and then ultrasonically etching them in Murakami solution for 1 min. The former reveals an apparently dense, ~3.5 μm thick diamond film on top of the granular substrate. The sequence of surface images recorded at progressively higher resolution indicates that the film has nucleated non-uniformly, forming a porous mesh structure that extends across the entire substrate surface. The pore density appears fairly uniform on the mesoscale, but the individual pores display a broad range of (irregular) shapes and sizes; the highest resolution image [Fig. 1(f)] confirms the surface morphology characteristic of polycrystalline diamond.

The Raman spectrum of a PD film deposited on a sintered WC-13 wt.%Co substrate [Fig. 2(a)] shows an obvious background that rises to higher wavenumber. This photoluminescence (PL) contribution is fitted using a linear function [also shown in Fig. 2(a)] and then subtracted to yield the Raman contributions, which are then fitted using a set of Lorentzian functions – as shown in Fig. 2(b). The decomposition identifies several peaks with different Raman shifts (at ~1140, 1332, 1355, 1470 and ~1575 cm^{-1}). The Raman spectrum shows an obvious diamond peak, centred at 1337.8 cm^{-1}. The peak is relatively broad (full width half maximum ~8.7 cm^{-1}) and rides on a background associated with graphitic (sp^2-bonded) carbon. The diamond peak is blue-shifted relative to its position in stress-free diamond (1332.2 cm^{-1}), suggesting the presence of some compressive stress in the deposited film – which is likely associated with the mismatch in thermal expansion between the substrate and the diamond film [21]. There is a growing body of evidence supporting sp^2 carbon based assignments for the ~1140 and 1470 cm^{-1} peaks [22, 23], though the former feature is still sometimes invoked as a signifier of a nanocrystalline diamond phase in as-grown CVD samples [24, 25].

The XRD pattern of a PD film grown on sintered WC-13 wt.%Co substrate [Fig. 2(c)] is dominated by WC features, but peaks at 2θ diffraction angles of 43.9°, 75.4° and 91.4° – corresponding to, respectively, the (111), (220) and (311) reflections of the cubic diamond structure – are clearly identifiable. Note that the 2θ ~75.4° peak matches

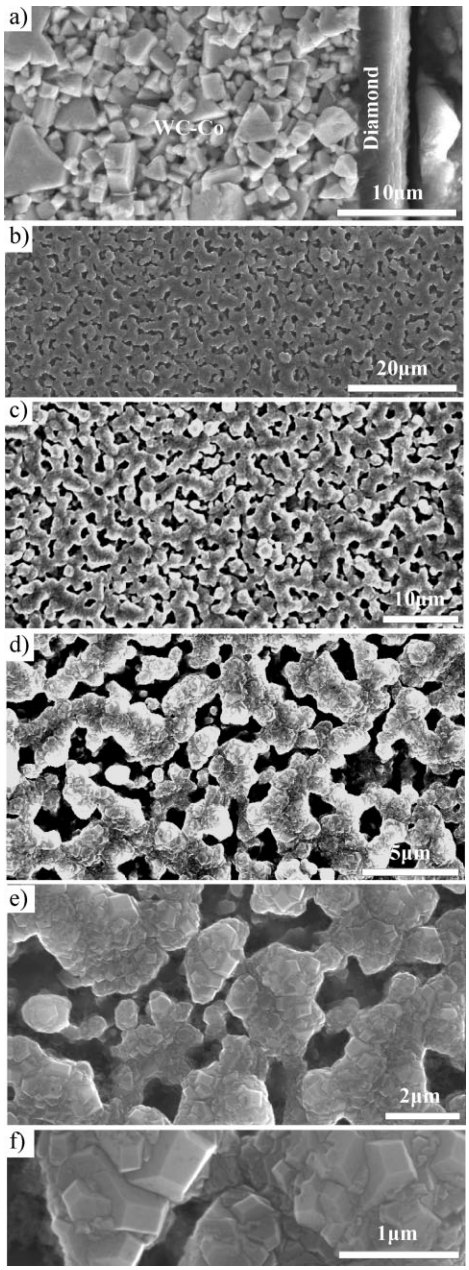

Figure 1 SEM images of PD films grown on a sintered WC-13 wt.%Co cemented carbide substrate. (a) Shows a cross-sectional image, (b)–(f) show plan view images recorded at successively higher resolutions.

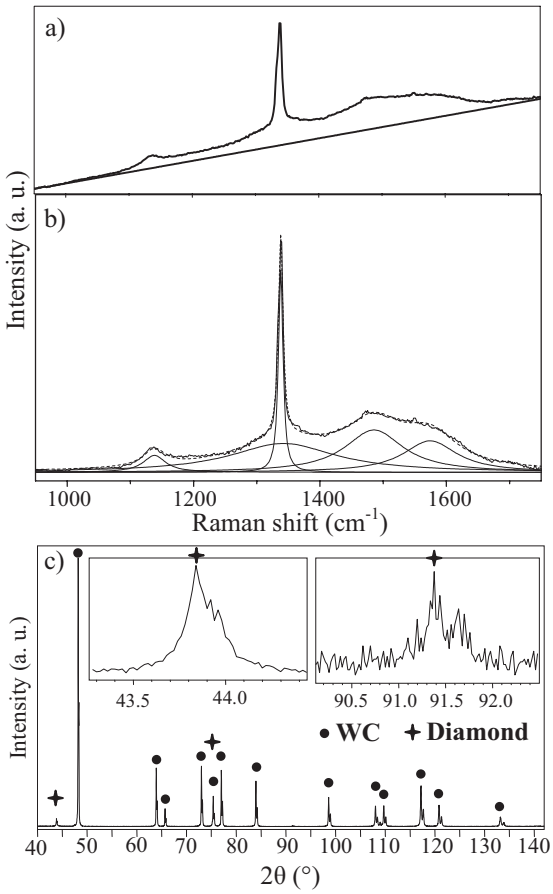

Figure 2 (a) Raman spectrum of a PD film grown on a sintered WC-13 wt.%Co cemented carbide substrate, along with a linear function showing the assumed PL background contribution. (b) 'Difference' spectrum obtained by subtracting the background contribution from the measured spectrum, together with its decomposition into a set of five Lorentzian functions. (c) XRD pattern of a PD film grown on a sintered WC-13 wt.%Co cemented carbide substrate. Expanded views of the reflections at $2\theta \sim 43.9^\circ$ and 91.4° are shown in the insets.

closely with the diamond (220) peak at 75.302° and the WC (200) peak at 75.477°; the observed feature is considered to be a blend of these two reflections.

The blue-shift of the diamond peak in the Raman spectrum [Fig. 2(a)] was taken as evidence that the PD films are under compressive stress – implying that the films are adhered to the underlying substrate. Figure 3 shows an SEM image of the indent in a PD film made with an applied load of 1500 N. We observe no flaking-off of the PD film around the indentation – reinforcing the conclusion that the PD film is well-adhered to the underlying WC substrate.

PD films grown on WC-Co substrates not dissimilar to those described here have been reported previously [26–28], but the formation mechanism of such films is still unclear. The porous structures in the present work were only observed with Ar present in the process gas mixture, with the application of an appropriate substrate bias voltage, and with a structured substrate surface. We now consider the likely role of these various factors.

We have shown previously that the MC pre-treatment used here results in a textured WC-Co substrate surface, especially with high-Co-containing cemented carbides [16]. This can be traced to the fact that cemented carbides are typically fabricated by powder metallurgy methods, wherein the Co binder distributes between the WC grains. The purpose of the first step of MC-treatment (*i.e.*, the etching of tungsten carbide by Murakami's reagent) is to increase the substrate surface roughness and to expose the Co binder

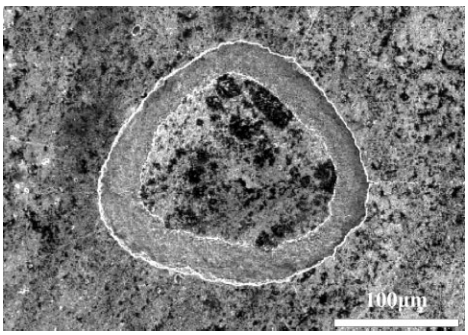

Figure 3 SEM image of a PD film grown on a sintered WC-13 wt.%Co cemented carbide substrate after Rockwell indentation with an applied load of 1500 N.

[as illustrated in Fig. 4(a)], thereby enhancing the efficiency of the second step of the MC pre-treatment during which Co is etched by the acidic solution of hydrogen peroxide, as illustrated in Fig. 4(b). MC pre-treatment thus creates a Co-deficient, loose, granular layer on the substrate surface suitable for subsequent diamond nucleation and growth [16, 27]. As such, these substrates show some parallels with the studies of Braga et al. [3–6] wherein hybrid three-dimensional (3-D) electrodes were formed by growing (by HFCVD) microcrystalline boron-doped diamond and/or nanocrystalline diamond films on porous Ti substrates.

The use of a negative bias during the early stages of diamond growth, as here, is a recognized route to enhancing nucleation. Bias-enhanced nucleation, wherein ions in the process gas mixture are accelerated towards and bombard the substrate surface is widely used in microwave plasma enhanced (MWPE) CVD to increase the nucleation density on, for example, mirror-polished silicon substrates [29]. HF activated gas mixtures generally contain a much lower (but

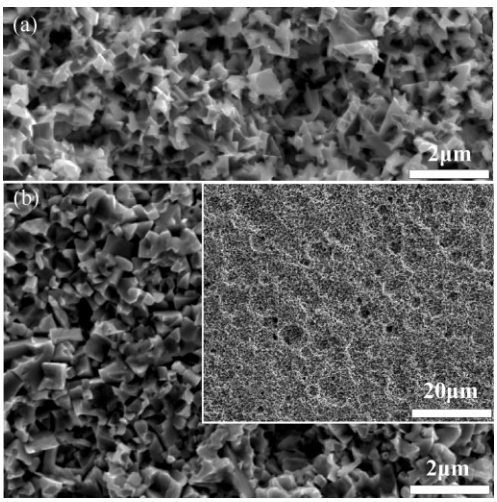

Figure 4 SEM images of the surface of a WC-13 wt.%Co cemented carbide substrate after (a) etching of tungsten carbide by Murakami's reagent and (b) etching of Co by the acidic solution of hydrogen peroxide. The inset shows a large region of the latter surface imaged at lower resolution.

non-zero) density of ions, formed by thermionic emission from the HF and subsequent electron-atom/molecule collisions in the gas phase. Malcher et al. were the first to report diamond film deposition on WC-Co tools using a double bias-assisted HFCVD system [30]. Chattopadhyay et al. have also investigated the effects of applying a direct current (DC) substrate bias (in the range $-500 \geq V_{DC} \geq -1500$ V) on the morphology and adhesion of diamond coatings grown on carbide turning tools using a modified HFCVD method [31]. Park et al. have reported more extensive and systematic investigations of the effect of different bias voltages (0, −80, −100 and −120 V) on the diamond grain size in films grown on 3-D WC-6 wt.%Co substrates [32]. Ion bombardment can induce defects on the surface of the growing diamond film, which act as sites for re-nucleation, thereby resulting in a smaller average grain size. Such effects were found to be most pronounced at the edges of a 3-D object, where the local electric field is greatest. Ižák et al. investigated the influence of nucleation time (30–120 min) at a constant substrate bias voltage and the influence of bias voltage (from −120 to −220 V) for a fixed nucleation time on the growth of diamond on silicon in a HFCVD reactor [33]. No diamond clusters were observed in SEM images of samples subjected to the shortest nucleation time, just very small (<10–20 nm) points of luminescence, but progressively more diamond clusters were evident at longer process times. A relatively homogeneous array of diamond clusters (with sizes in the range 50–100 nm and a density $\sim 10^8$ cm^{-2}) was evident after 60 min. Extending the process time further was found to result in continued expansion of the diamond clusters (to ~100–130 nm) and an apparent reduction in cluster density (to $\sim 10^7$ cm^{-2}). The studies in which V_{DC} was varied while maintaining a constant nucleation time yielded similar trends; larger negative bias voltages resulted in larger diamond clusters.

Applying a positive substrate bias cannot lead to an increased diamond nucleation density from positive ion imapcts. Yet the present study finds that such a bias at later time ($t > 45$ min) has a beneficial effect on diamond film growth. Saito et al. have concluded that the main effects of the positive bias during MWPE-CVD of diamond are (i) suppression of ion bombardment on the growing diamond surface (which might otherwise induce surface damage and secondary nucleation) and (ii) an increase in the rate of electron impact, which can enhance radical formation on the growing diamond surface (especially in the case of (100) oriented diamond grains) [34].

Finally, we address the role of the Ar. Addition of just a few percent of Ar (as here) cannot have any major effect on the thermal diffusion or heat transport in the gas. Rather, the addition of Ar is assumed to increase the density of heavy ions impacting on the substrate surface at early times. The electron density, and thus the probability of energetic electron-Ar collisions, will be highest near the HF. Ions formed in this region will be driven towards the substrate by a negative bias voltage. Yang et al. have investigated the

combined effects of Ar addition and substrate bias on the growth-rate, grain-size, and morphology of diamond films [35], and suggested that substrate biasing enhances the production of H^+ and Ar^+ ions, thereby influencing surface etching and subsequent diamond film growth. Ansari et al. explored the effect of substrate bias on the growth kinetics of diamond films by HFCVD using CH_4/H_2 mixtures diluted with 7%Ar [36]. Ar addition was found to increase the nucleation density and growth rate, leading to suggestions that excited noble gas atoms and ions aid the excitation and dissociation of hydrogen and/or hydrocarbon molecules – thereby boosting the number densities of key growth species. Csikvari et al. have also studied the effect of substrate bias on the morphology and microstructure of diamond layers formed by MWPE-CVD using $H_2/CH_4/Ar$ gas mixture containing Ar fractions ranging from 10–95% [37]. Ar-dependent variations in the gas phase chemistry and composition of such MW activated $H_2/CH_4/Ar$ gas mixtures have been investigated also – by *in situ* mass spectrometry of the ionic species [34] and by laser absorption and optical emission spectroscopy [38].

4 Conclusions In this work, we have established optimal CVD conditions for growing high quality, adherent, PD films on sintered WC-13 wt.%Co substrates in a HFCVD system. The detailed formation mechanism of PD films on WC-13 wt.%Co substrates is still unclear, but porous structures such as those reported in the present work are only observed with Ar present in the process gas mixture, with the application of an appropriate substrate bias voltage during the early stages of deposition, and with a structured substrate surface.

Acknowledgements We gratefully acknowledge the China Scholarship Council, the State Key Laboratory of Powder Metallurgy, and the Outstanding PhD Students Enabling Fund and Open Fund for Valuable Instruments of Central South University for financial support.

References

[1] Y. Takano, J. Phys.: Condens. Matter **21**, 253201 (2009).
[2] J. H. T. Luong, K. B. Male, and J. D. Glennon, Analyst **134**, 1965 (2009).
[3] N. A. Braga, C. A. A. Cairo, J. T. Matsushima, M. R. Baldan, and N. G. Ferreira, J. Solid State Electrochem. **14**, 313 (2010).
[4] N. A. Braga, C. A. A. Cairo, N. G. Ferreira, M. R. Baldan, and V. J. Trava-Airoldi, Diamond Relat. Mater. **19**, 764 (2010).
[5] N. A. Braga, C. A. A. Cairo, E. C. Almeida, M. R. Baldan, and N. G. Ferreira, Diamond Relat. Mater. **18**, 1065 (2009).
[6] N. A. Braga, C. A. A. Cairo, E. C. Almeida, M. R. Baldan, and N. G. Ferreiraa, Diamond Relat. Mater. **17**, 1891 (2008).
[7] S. K. Arora, S. Chhoker, N. K. Sharma, V. N. Singh, and V. D. Vankar, J. Appl. Phys. **104**, 103524 (2008).
[8] A. Glaser, S. M. Rosiwal, and R. F. Singer, Diamond Relat. Mater. **15**, 49 (2006).
[9] Y. C. Chen, C. Y. Chen, N. H. Tai, Y. C. Lee, S. J. Lin, and I. N. Lin, Diamond Relat. Mater. **15**, 324 (2006).
[10] G. H. Chen, R. Q. Cai, X. M. Song, and J. X. Deng, Mater. Sci. Eng. B **107**, 233 (2004).
[11] A. V. Karabutov, S. K. Gordeev, V. G. Ralchenko, S. B. Korchagina, S. V. Lavrischev, S. V. Terekhov, K. I. Maslakov, and A. P. Dementjev, Diamond Relat. Mater. **12**, 1710 (2003).
[12] V. Baranauskas, A. C. Peterlevitz, D. C. Chang, and S. F. Durrant, Appl. Surf. Sci. **185**, 108 (2001).
[13] Q. Wei, Z. M. Yu, M. N. R. Ashfold, Z. Chen, L. Wang, and L. Ma, Surf. Coat. Technol. **205**, 158 (2010).
[14] Q-p. Wei, Z. M. Yu, M. N. R. Ashfold, L. Ma, and Z. Chen, Diamond Relat. Mater. **19**, 1144 (2010).
[15] Q. P. Wei, Z. M. Yu, L. Ma, D. F. Yin, and J. Ye, Appl. Surf. Sci. **256**, 1322 (2009).
[16] Q-p. Wei, Z. M. Yu, M. N. R. Ashfold, J. Ye, and L. Ma, Appl. Surf. Sci. **256**, 4357 (2010).
[17] Z. Yu, U. Karlsson, and A. Flodstrom, Thin Solid Films **342**, 74 (1999).
[18] M. G. Peters and R. H. Cummings, European Patent 0519587 A1 (1992).
[19] D. Das and R. N. Singh, Inter. Mater. Rev. **52**, 29 (2007).
[20] H. Liu and D. S. Dandy, Diamond Relat. Mater. **4**, 1173 (1995).
[21] V. F. Neto, R. Vaz, N. Ali, M. S. A. Oliveira, and J. Gracio, Diamond Relat. Mater. **17**, 1424 (2008).
[22] A. C. Ferrari and J. Robertson, Phys. Rev. B **63**, 121405 (2001).
[23] R. Pfeiffer, H. Kuzmany, P. Knoll, S. Bokova, N. Salk, and B. Günther, Diamond Relat. Mater. **12**, 268 (2003).
[24] X. M. Meng, S. J. Askari, W. Z. Tang, L. F. Hei, F. Y. Wang, C. S. Jiang, and F. X. Lu, Vacuum **82**, 543 (2008).
[25] A. Schneider, D. Steinmueller-Nethl, M. Roy, and F. Franek, Int. J. Refract. Met. H. Mater. **28**, 40 (2010).
[26] R. Polini, Thin Solid Films **515**, 4 (2006).
[27] C. L. Geng, W. Z. Tang, L. F. Hei, S. T. Liu, and F. X. Lu, Inter. J. Refract. Metal H. Mater. **25**, 159 (2007).
[28] M. Gowri, W. J. P. van Enckevort, J. J. Schermer, J. P. Celis, J. J. ter Meulen, and J. G. Buijnsters, Diamond Relat. Mater. **18**, 1450 (2009).
[29] S. Yugo, T. Kanai, T. Kimura, and T. Muto, Appl. Phys. Lett. **58**, 1036 (1991).
[30] V. Malcher, A. Mrska, A. Kromka, A. Satka, and J. Janik, Curr. Appl. Phys. **2**, 201 (2002).
[31] A. Chattopadhyay, S. K. Sarangi, and A. K. Chattopadhyay, Appl. Surf. Sci. **255**, 1661 (2008).
[32] J. K. Park, W. S. Lee, Y. J. Baik, and K. W. Chae, Diamond Relat. Mater. **12**, 1657 (2003).
[33] T. Ižák, M. Marton, M. Varga, M. Vojs, M. Vesely, R. Redhammer, and M. Michalka, Vacuum **84**, 49 (2009).
[34] D. Saito, H. Isshiki, and T. Kimura, Diamond Relat. Mater. **18**, 56 (2009).
[35] T. S. Yang, J. Y. Lai, M. S. Wong, and C. L. Cheng, J. Appl. Phys. **92**, 4912 (2002).
[36] S. G. Ansari, T. L. Anh, H. K. Seo, K. G. Sung, D. Mushtaq, and H. S. Shin, J. Cryst. Growth **265**, 563 (2004).
[37] P. Csikvari, A. Somogyi, M. Veres, G. Hars, and A. Toth, Diamond Relat. Mater. **18**, 1459 (2009).
[38] J. C. O. Richley, J. L. Fox, M. N. R. Ashfold, and Y. A. Mankelevich, J. Appl. Phys. **109**, 063307 (2011).